International Journal of Cardiology 292 (2019) 148–155

Contents lists available at ScienceDirect

International Journal of Cardiology

journal homepage: www.elsevier.com/locate/ijcard

Left atrial microvascular endothelial dysfunction, myocardial inflammation and fibrosis after selective insular cortex ischemic stroke☆

Brittany Balint [a,b,c,1], Victoria Jaremek [a,b,c,1], Victoria Thorburn [a,b,c], Shawn N. Whitehead [a,b,c,2], Luciano A. Sposato [b,c,d,e,f,g,*,2]

[a] Vulnerable Brain Laboratory, Department of Anatomy and Cell Biology, Schulich School of Medicine and Dentistry, Western University. 339 Windermere Rd, London, ON N6A 5A5, Canada
[b] Heart & Brain Laboratory, Western University, 339 Windermere Rd, London, ON, N6G 5A5, Canada
[c] Department of Anatomy and Cell Biology, Schulich School of Medicine and Dentistry, Western University, 339 Windermere Rd, London, ON N6A 5A5, Canada
[d] Department of Clinical Neurological Sciences, London Health Sciences Centre, Schulich School of Medicine and Dentistry, Western University, 339 Windermere Rd, London, ON N6A 5A5, Canada
[e] Department of Epidemiology & Biostatistics, Schulich School of Medicine & Dentistry, Western University, 339 Windermere Rd, London, ON N6A 5A5, Canada
[f] Robarts Research Institute, Schulich School of Medicine and Dentistry, Western University, 1151 Richmond St. N., London, ON N6A 5B7, Canada
[g] Lawson Research Institute, 750 Base Line Rd E, London, ON N6C 2R5, Canada

ARTICLE INFO

Article history:
Received 18 April 2019
Received in revised form 15 May 2019
Accepted 1 June 2019
Available online 2 June 2019

Keywords:
Stroke
Myocardial inflammation
Myocardial fibrosis
Arrhythmia
Coronary microvascular endothelial dysfunction

ABSTRACT

Background: Insular cortex (IC) ischemic strokes are associated with increased risk of cardiac arrhythmias. We have previously hypothesized that the anatomical substrate for post-stroke neurogenic arrhythmias comprises stroke-induced left atrium (LA) coronary microvascular endothelial dysfunction (CMED), and myocardial inflammatory infiltration (MII) leading to myocardial fibrosis. We investigated whether selectively induced IC ischemic stroke in rats results in histopathological changes in the LA.

Methods: Insular ischemic stroke was induced in 6-month old male Wistar rats via unilateral stereotaxic injection of endothelin-1 into the left or right IC. The control group consisted of rats injected with saline. We histologically examined the LA 28 days after stroke for CMED, MII, and fibrosis. We performed linear regression analyses to assess correlation between the 3 histopathological outcomes. We compared these findings in the distal LA and the LA-pulmonary vein border (LA-PV border), a region of rich autonomic innervation.

Results: Right and left IC stroke led to CMED, MII, and fibrosis in the LA. MII was significantly correlated with CMED and fibrosis. The LA-PV border had significantly greater MII and fibrosis than the distal LA. There were no differences in coronary microvascular and myocardial changes between left and right IC strokes.

Conclusions: Left and right insular ischemic strokes resulted in CMED, MII, and fibrosis, the pathological hallmark of arrhythmogenic LA tissue. Since these changes were greater within the LA-PV border than in the distal LA tissue, the role of preganglionic fibers at the ganglionated plexi as part of neurogenic arrhythmogenesis warrants further investigation.

1. Introduction

Atrial fibrillation is newly diagnosed in up to 24% of patients after an acute ischemic stroke [1]. We have recently hypothesized that acute ischemic damage to the insular cortex results in autonomic surges and systemic and local inflammatory responses [2] with the potential to trigger neurogenic atrial fibrillation [3].

Our hypothesis suggests that insular cortex infarcts are associated with systemic inflammation and autonomic dysregulation [2]. Post-stroke autonomic dysregulation increases systemic [4] and local catecholamine release from myocardial nerve endings [5] following sympathetic overactivation [6], ultimately precipitating left atrial (**LA**) myocardial inflammatory infiltration (**MII**) [7]. Additionally, in response to pro-inflammatory mediators, microvascular endothelial cells become inappropriately activated, resulting in coronary microvascular endothelial dysfunction (**CMED**) further perpetuating the inflammatory process [8,9]. In turn, recruitment of lymphocytes within the myocardium contribute to myocardial fibrosis [10,11]. As such, LA fibrosis is enhanced by CMED and chronic MII [12]. Eventually, the excess fibrosis, pathological hallmark of arrhythmogenic LA tissue, results in atrial fibrillation

☆ All authors take responsibility for all aspects of the reliability and freedom from bias of the data presented and their discussed interpretation.

* Corresponding author at: Room A10-322 UH, 339 Windermere Road, London, ON N6A 5A5, Canada.
E-mail address: Luciano.Sposato@LHSC.on.ca (L.A. Sposato).

[1] Equal contributions as lead authors.
[2] Equal contributions as senior authors.

https://doi.org/10.1016/j.ijcard.2019.06.004
0167-5273/

generation and perpetuation [13]. To date, LA CMED, MII, and fibrosis have not been investigated in rat models of ischemic stroke or in humans.

The functional lateralization of the insular cortex adds complexity to the understanding of neurogenically mediated LA injury. Clinical reports have correlated insular ischemic stroke with worse cardiovascular outcomes [14,15], possibly caused by ischemic damage to the right insular cortex. However, the role of the lateralization of the insular cortex in stroke-related LA injury remains controversial and needs to be investigated.

Another challenge related to the characterization of LA injury post-stroke is the identification of reliable biomarkers with the potential to be used in human research and clinical practice. Among potential candidate biomarkers, brain natriuretic peptide [16], troponin T [17], and LA enlargement [18] have been associated with cardiac fibrosis [19] and constitute the most widely used blood and echocardiographic markers. Despite this, their correlation with definite post-stroke LA coronary microvascular and myocardial injury remains unproven.

We hypothesized that LA CMED, MII, and fibrosis would be greater in rats with endothelin-1 (**ET-1**) induced selective right and left insular cortex ischemic stroke than among a control group undergoing injection of phosphate-buffered saline (**PBS**). Additionally, based on prior evidence suggesting that myocardial changes after stroke are most substantial in the periphery of myocardial nerve endings [20] and that the border between the LA and the pulmonary vein (**LA-PV border**) is a region of high autonomic innervation [21], we hypothesized that the LA-PV border would show more severe changes than more distal LA regions. We therefore compared the extent of CMED, MII, and fibrosis at the LA-PV border and at the distal LA. With the purpose of identifying biomarkers to be used in humans, we compared brain natriuretic peptide, troponin T, and left atrial size among rats with ET-1 induced insular stroke and controls.

2. Methods

2.1. Animals

Twenty-six male Wistar rats aged 6 months and weighing 500–600 g were randomly assigned to either the insular stroke group (left: $n = 7$, right: n = 7) or the PBS control group (left: $n = 6$, right: n = 6). Brain natriuretic peptide and troponin T analyses involved 22 male Wistar rats that were randomly assigned to either the insular stroke group (left: $n = 5$, right: $n = 6$) or the PBS control group (left: n = 5, right: n = 6).

2.2. ET-1 induced insular cortex ischemic stroke

Insular cortex ischemic stroke was induced by unilateral injection of ET-1 into either the left ($n = 7$) or right (n = 7) insular cortex. Control rats received a unilateral injection of PBS (left: $n = 6$, right: n = 6). Surgery was performed with isoflurane anesthetic (Baxter Corporation, Mississauga, Canada; 4% with 2.0 L/min of oxygen for induction, shifted to 2% isoflurane once in surgical plane). Prior to surgery, 0.03 mg/kg buprenorphine diluted in 0.9% sterile sodium chloride was administered subcutaneously. Anaesthetized rats were secured in a Kopf stereotaxic frame and a single injection of ET-1 (20 pmol dissolved in 1 μL sterile 0.9% saline) was performed unilaterally over 5 min into the insular cortex (AP: −1.0 mm, ML: ±6.5 mm, DV: −7.0 mm relative to bregma) using a 32-guage Hamilton syringe (Hamilton Company, Reno, NV). Control rats that were injected with equal volume of PBS underwent identical procedures with equivalent time under isoflurane anesthesia. All rats were euthanized 28 days after surgery, transcardially perfused with 0.01 M PBS, followed by 4% paraformaldehyde. Brain and cardiac tissue were extracted and temporarily stored in 4% PFA at 4 °C for 24 and 48 h, respectively. Brain tissue was then transferred to 30% sucrose and stored at 4 °C until sectioned. The heart was dehydrated in ethanol/water series, cleared in xylene and embedded in 65 °C paraffin wax.

2.3. Brain histology and immunohistochemistry

Brain tissue was flash frozen in Tissue-Tek™ O.C.T. Compound (Sakura Finetek USA Inc., Torrance, CA) and sectioned into 35 μm coronal sections using the CryoStar NX50 cryostat (Thermo Fisher Scientific, Waltham, MA). To qualitatively analyze insular injury, 2× and 20× photomicrographs of the right and left insular cortices stained with thionin, OX-6 (Lot 554,926; BD Biosciences, Mississauga, ON), and NeuN (Lot MAB377; Sigma-Aldrich, Oakville, ON) were taken. Thionin indicated presence of healthy cell populations, OX-6 was used to identify activated microglia within the insular cortex, and NeuN confirmed neuronal loss.

2.4. Histochemistry and immunohistochemistry for LA CMED, MII, and fibrosis

Endothelial cell function in atrial coronary microvessels was detected by immunohistochemistry with an antibody that recognizes phosphorylated eNOS (rabbit anti-eNOS, Ser1177, GTX50212, 1:50; GeneTex, Irvine, California, USA). Tissue sections were incubated in primary antibody for 1 h at room temperature. Following 3 × 15 min washes in PBS, sections were incubated for 1 h at room temperature with the appropriate biotinylated secondary antibody (goat anti-mouse, goat anti-rabbit biotinylated antibodies, 1:500, Vector Labs, Burlington, ON, Canada). Following 3 × 15 min washes in PBS, sections were incubated with avidin biotin complex and daminobenzadine (Vector Labs, Burlington, ON, Canada). Sections were then counterstained using Harris' Hematoxylin. Immunostaining on 5 μm thick tissue sections was also performed for B-lymphocytes (mouse anti-CD45R, HIS24; sc-19,615, 1:100; Santa Cruz Biotechnology, California, USA), T-lymphocytes (rabbit anti-CD3, ab16669, 1:200; Abcam, Cambridge, MA, USA), neutrophils (rabbit anti-myeloperoxidase, MPO, ab9537, 1:100; Abcam, Cambridge, MA, USA), and leukocytes (rabbit anti-CD45, ab10558, 1:200; Abcam, Cambridge, MA, USA). To detect tissue fibrosis, 5 μm sections of the LA were stained with Masson's trichrome [22].

Stroke and catecholamine surges have been associated with myocytolysis, in which myocytes die in a hypercontracted state [23,24]. To assess whether fibrosis was mediated by myocytolysis, 5 μm sections were stained with H&E [22].

2.5. Image analyses

All histological analyses were performed by two investigators blinded to experimental group identities. All images were acquired using a Nikon Eclipse Ni—U upright microscope with a DS-Fi2 high definition colour camera and imaging software (NIS Elements, Melville, NY, USA), and ImageJ (Version 1.45; National Institute of Health, Bethesda, MD) was used for all image analysis.

For LA fibrosis measurements, 8 regions of interest were chosen for both the distal LA and LA-PV border. The area of fibrosis for each regions of interest was measured by isolating the blue colour channel using colour deconvolution in ImageJ. Fibrosis was defined as the fraction of blue within the total cellular area imaged. For CD3, CD45, CD45R. MPO and eNOS stained tissue sections, cells were counted in each region of interest ($n = 5$ per rat) and cell counts were averaged for each individual rat and expressed as positive cells per myocyte area. To quantify endothelial dysfunction, 10 blood microvessels from phosphorylated eNOS stained tissue, were randomly chosen per region and imaged at 40× magnification. Positive eNOS endothelial cells were quantified and expressed to the total endothelial cells in each blood vessel.

To assess whether the pathological cardiac consequences of selective insular stroke were more prominent in regions of autonomic innervation, findings in the LA-PV border [21] were compared to those in the distal LA tissue. We imaged 5 regions of interest from the distal LA and LA-PV border at 20× magnification. We counted the number of positive cells and normalized the results to the myocyte area (μm^2).

2.6. ELISA for time-course of brain natriuretic peptide and troponin T

Venous blood samples from time-course rats were collected in EDTA tubes (Microvette® CB 300 K2E, Sarstedt, Nümbrecht, Germany) at baseline (0 h), 6 h, 24 h, 7d, 14d and 28d following ET-1 or PBS injections. The samples were centrifuged and stored at −80 °C until analysis. Plasma levels of BNP were measured using BNP 45 (abcam ab108816) in vitro ELISA following manufacturer protocols. They were analyzed using a microplate reader (Epoch™ Microplate Spectrophotometer, BioTek Instruments, Winooski, VT, United States) with Gen5 Microplate Reader Software (BioTek Instruments). Troponin T plasma levels were evaluated via Milliplex Rat Cardiac Injury Magnetic Bead Panel 1, RCI1MAG-87 K (Millipore Corporation, Billerica, MA) using the protocols recommended by the manufacturer. Levels were analyzed using a Bio-PlexTM 200 readout System (Bio-Rad Laboratories, CA, United States) via Luminex® xMAPTM multiplex immunoassay technology (Luminex Corp., TX, United States). Troponin T levels were automatically calculated from standard curves using Bio-Plex Manager software (v.4.1.1, Bio-Rad).

2.7. Measurement of LA size

To measure LA area and diameter, 5 μm sections were stained with H&E [22]. LA area and diameter were quantified using selection tool in ImageJ.

2.8. Statistics

Surgical group values are expressed as mean ± standard error of the mean. All statistical analyses were performed using GraphPad Prism (GraphPad, La Jolla, CA). All data sets passed assessment of normality (D'Agostino and Pearson omnibus normality test). Means were compared using either Student's *t*-test or two-way ANOVA with Bonferroni post hoc tests. To determine whether a relationship existed between the level of inflammation and the extent of cardiac fibrosis and endothelial cell dysfunction in response to selective insular stroke, linear regression analyses were performed.

2.9. Study approval

All procedures involving live animals were conducted in accordance with the Canadian Council for Animal Care guidelines and approved by the Animal Care Committee at the University of Western Ontario (protocol number: 2016–027).

3. Results

3.1. Precision of ET-1 induced insular strokes

OX-6 staining showed targeted neuroinflammation in either left or right insular cortex 28 days post-stroke (Supplemental Fig. 1A). Thionin, NeuN and OX-6 staining revealed loss of Nissl bodies, neuronal loss, and activated pro-inflammatory microglia within the left or right insular cortex following stroke induction (Supplemental Fig. 1B).

3.2. Coronary microvascular endothelial dysfunction

There was increased immunostaining of eNOS in endothelial cells in the LA (Fig. 1A) after left ($P = 0.04$) and right ($P = 0.004$) selective insular stroke compared to the right and left PBS groups (Fig. 1B). No differences were observed between the left and right insular stroke groups (Fig. 1B).

3.3. Left atrial myocardial inflammatory infiltration

CD45, a pan-leukocyte marker, was significantly increased in the LA of rats with left ($P = 0.0009$, Fig. 3A) or right ($P = 0.0004$; Fig. 2A) insular cortex stroke compared to those with left and right PBS injection, respectively. There were no differences in the level of pan-leukocyte infiltration following left or right insular cortex ischemic stroke and left or right PBS injection ($P = 0.1$). Neutrophil recruitment was significantly higher in left ($P = 0.02$, Fig. 2B) and right IC ($P = 0.04$; Fig. 2B) stroke rats than in those with PBS injection. T lymphocyte infiltration was increased in the LA of both left ($P < 0.0001$, Fig. 2C) and right ($P = 0.0003$; Fig. 2C) insular cortex stroke rats compared to their PBS counterparts. Similarly, B lymphocyte infiltration was higher in the LA following ET-1 injection into either the left ($P = 0.011$; Fig. 2D) or right IC ($P = 0.0006$; Fig. 2D) than after PBS injection at 28 days post-stroke.

3.4. Left atrial fibrosis

Masson's trichrome staining revealed extensive collagen deposition in the form of interstitial fibrosis in rats that received ET-1 injection into either the left ($P = 0.02$; Fig. 3A and B) or the right insular cortex ($P = 0.02$; Fig. 3A and B) compared to PBS injected rats at 28 days after stroke. The extent of cardiac fibrosis was the same regardless of which insular hemisphere was impacted by the stroke ($P = 0.63$).

3.5. Correlation between left atrial inflammation, coronary microvascular endothelial dysfunction and fibrosis

Understanding that LA inflammation could predispose to local fibrosis, we sought to determine whether a relationship exists between the level of inflammation and the extent of cardiac fibrosis in response to selective insular stroke. Linear regression analysis revealed that the level of LA leukocyte infiltration and the amount of LA fibrosis 28 days following stroke induction were significantly correlated ($R^2 = 0.3967$, $P = 0.0158$; Supplemental Fig. 2A). Considering our hypothesis suggesting that CMED may enhance MII, we assessed the correlation between both histopathological changes. A significant correlation between the level of leukocyte infiltration and the amount of phosphorylated eNOS-expressing endothelial cells was found at 28 days after the insular stroke ($R^2 = 0.5747$, $P = 0.0007$; Supplemental Fig. 2B).

3.6. Increased inflammation and fibrosis at the left atrial-pulmonary vein border compared to the distal left atrium

Among insular cortex ischemic stroke rats, the LA-PV border revealed a significant increase in the proportion of fibrotic area compared to that observed in distal regions of the LA in the same group ($P = 0.0102$; Fig. 4A). However, this was not observed among control animals ($P = 0.7602$; Fig. 4A). Likewise, the number of CD45 positive cells was significantly increased at the LA-PV border compared to distal regions of the LA in rats with stroke ($P = 0.0180$; Fig. 4B), but there were no differences among PBS rats ($P = 0.7160$; Fig. 4B). No significant differences were observed in the proportion of activated eNOS-expressing endothelial cells in regions of high autonomic nervous system innervation compared to the distal LA after stroke ($P = 0.4927$; Fig. 4C) or in rats injected with PBS (Fig. 4C).

3.7. Plasma levels of brain natriuretic peptide and troponin T, and left atrial size

No significant differences were found in the time-course analysis (6 h, 24 h, 7 days, 14 days, and 28 days) of brain natriuretic peptide (Supplemental Fig. 3A) and troponin T (Supplemental Fig. 3B) following left or right selective insular stroke compared to left or right PBS groups. No differences were observed in LA diameter after left ($P = 0.61$) or

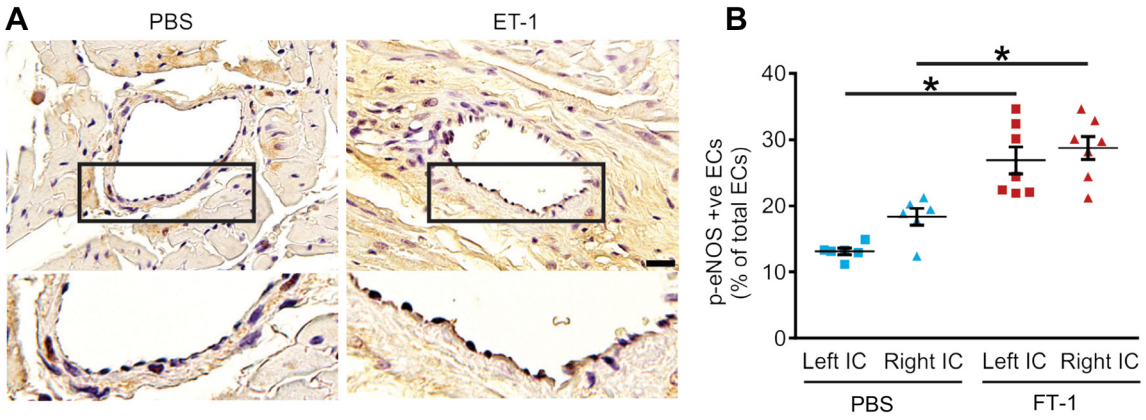

Fig. 1. eNOS activation in left atrial coronary microvessels. (A) Representative photomicrographs of coronary microvessels within LA tissue 28 days following PBS injection or ET-1 induced insular stroke, and immunostained for phosphorylated eNOS (p-eNOS; DAB). Nuclei were counterstained with hematoxylin. Scale bar = 100 μm. (B) Quantitative analysis revealed that the proportion of eNOS-activated endothelial cells was significantly increased following insular stroke. Data is represented as group mean ± SEM; *indicates statistical significance, $p < 0.05$, via two-way ANOVA, Bonferroni post hoc tests, $n = 6$–7 per experimental group.

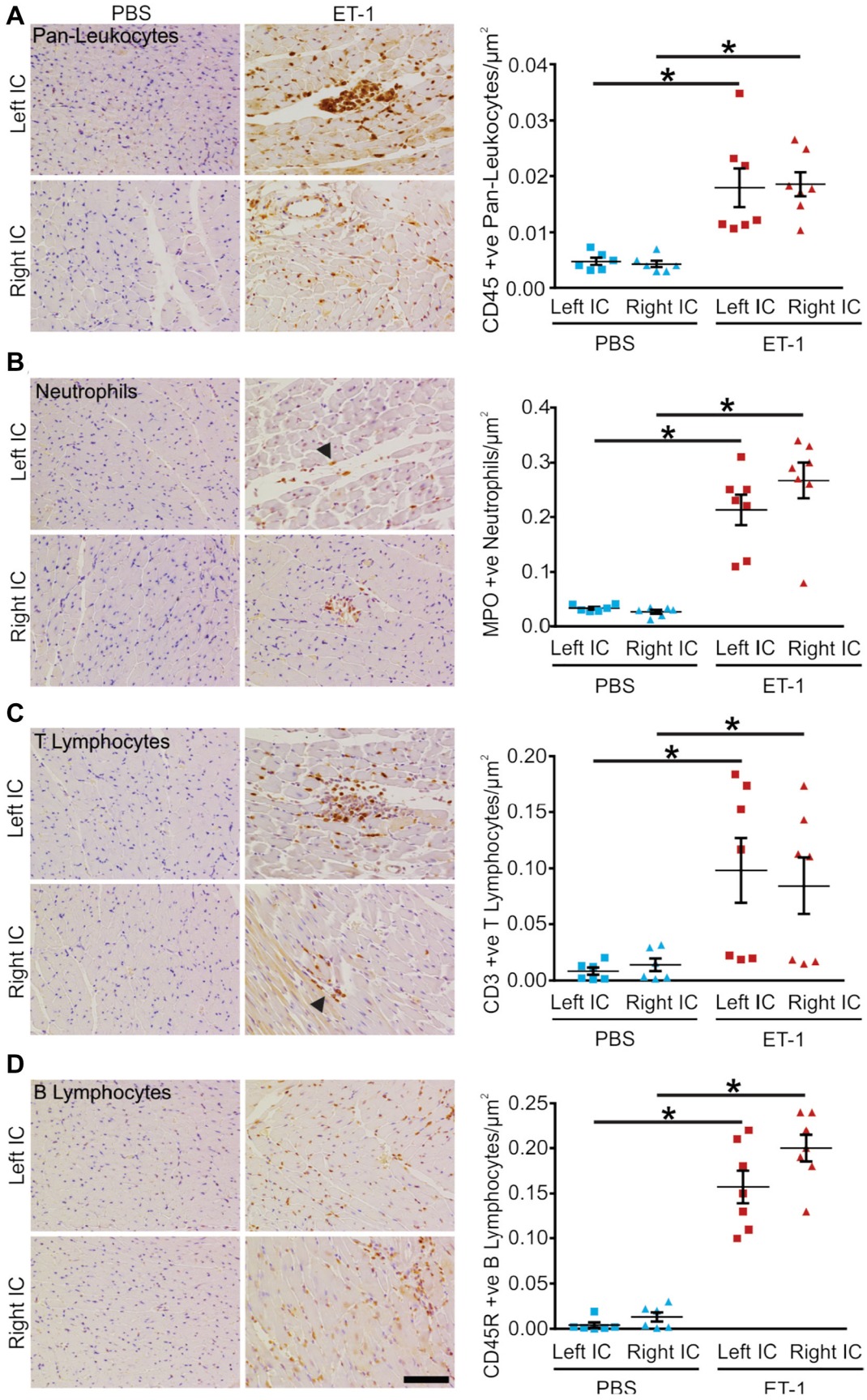

Fig. 2. Left atrial myocardial inflammatory infiltration. Representative photomicrographs of LA tissue harvested 28 days following PBS injection or ET-1 induced insular stroke ($n = 14$) and immunostained for inflammatory cell markers (left), with corresponding quantitation (right). LA tissue was immunostained for (A) pan-leukocytes (CD45), (B) neutrophils (myeloperoxidase, MPO), (C) T-lymphocytes (CD3) and (D) B-lymphocytes (CD45R). Nuclei were counterstained with hematoxylin. Data is represented as group mean ± SEM; *indicates statistical significance, $p < 0.05$, via two-way ANOVA, Bonferroni post hoc tests, n = 6–7 per experimental group. Scale bar = 50 µm.

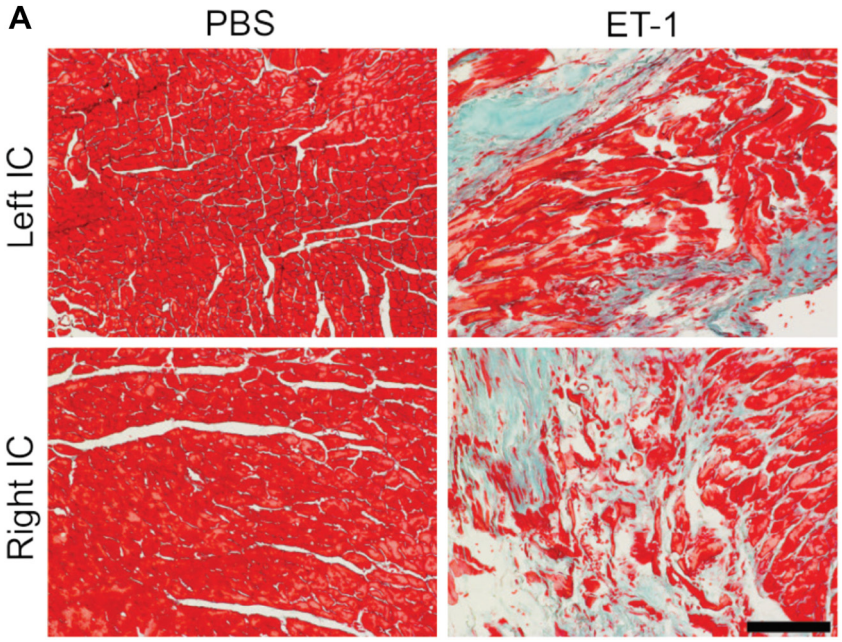

Fig. 3. Increased left atrial fibrosis. (A) Representative photomicrographs of LA tissue harvested 28 days following PBS injection or ET-1 induced insular stroke and stained with Masson's Trichrome stain. Blue stain labels collagen, and excessive collagen abundance indicates fibrotic regions. Scale bar = 100 μm. (B) Quantitative analysis revealed significantly increased LA fibrosis following selective insular stroke in left ($n = 7$; $P = 0.02$ vs. PBS) or right IC (n = 7; $P = 0.02$ vs. PBS). PBS: Phosphate-buffered saline (vehicle control; $n = 12$); LA: left atrium. Data is represented as group mean ± SEM; *indicates statistical significance, $p < 0.05$, via two-way ANOVA, Bonferroni post hoc tests.

right ($P = 0.35$) selective insular stroke compared to the right and left PBS groups (Supplemental Fig. 3C). Likewise, there were no differences in LA area in rats that received ET-1 injection into either the left ($P > 0.99$) or the right insular cortex ($P > 0.99$) compared to PBS injected rats (Supplemental Fig. 3D).

3.8. Absence of left atrial myocytolysis

No evidence of LA myocytolysis was seen in either the control or insular stroke rats (Supplemental Fig. 4).

4. Discussion

In a novel rat model of selective right and left insular ischemic stroke, brain infarcts accurately targeting the insular cortex caused significant CMED, MII, and fibrosis in the LA at 28 days after induction. We also found that LA MII and fibrosis were more prominent in the LA-PV border than in the more distal LA tissue. There were no differences in brain natriuretic peptic and troponin T levels or in LA area or diameter between left and right insular cortex strokes. To the best of our knowledge, this is the first animal model showing the role of selective insular cortex ischemic stroke as a cause of LA CMED, MII, and fibrosis.

Assessing for evidence of coronary microvascular changes in the LA, we found that the proportion of activated endothelial cells was significantly increased in stroke rats compared to control animals, which is an indication of CMED. Coincidentally with the persistence of neutrophils at 28 days, endothelial cell activation was increased 28 days following stroke induction, denoting chronic activation. Impairment of the inflammatory reflex could play a role in endothelial dysfunction, resulting in chronic up-regulation further enhancing eNOS phosphorylation [25]. In favor of this hypothesis, we found that LA pan-leukocyte infiltration was strongly correlated with eNOS activation in endothelial cells of coronary microvessels.

Endothelial dysfunction and inflammation are closely associated. Inflammatory cell infiltration appears to play a role in various types of cardiovascular injuries, including atherosclerosis, myocardial infarction, and heart failure [26]. The increased recruitment of neutrophils into the LA among insular stroke rats suggests that dysregulated endothelial cell activation may allow for rapid neutrophil infiltration via the vascular endothelium. As well, neutrophils themselves can promote endothelial damage via release of proteins and protease [27]. Notably, neutrophils were still increased at 28 days following stroke induction, indicating the perpetuation of acute inflammatory mechanisms. It has been proposed that autonomic dysfunction induced by insular damage could lessen the protective effects of the inflammatory reflex against the perpetuation of the inflammatory response [28]. Therefore, the impairment of the inflammatory reflex could explain why local neutrophilic inflammation persisted in the LA of stroke rats at 28 days. Importantly, inflammation is part of the pathophysiology of neurogenic atrial fibrillation detected after stroke (AFDAS) [29]. Indeed, Acampa et al., have shown that elevated hypersensitive C reactive protein is associated with increased P wave dispersion, a well-recognized electrocardiographic marker of atrial fibrillation [30].

Insular cortex strokes resulted in increased LA fibrosis. This is consistent with early studies, in which cardiac pathological changes were observed at the histological level in post-mortem analyses of patients with cerebrovascular events [4,31]. However, most human studies were conducted among individuals with intracranial hemorrhage rather with ischemic stroke [31] and the majority of animal models of ischemic stroke were based on the occlusion of the middle cerebral artery instead of selectively targeting the insular cortex [4]. Inflammation is likely causative in the process of fibrotic remodeling of the myocardium [32]. Furthermore, inflammatory cells typically release cytokines that induce the activation and proliferation of cardiac fibroblasts, causing increased deposition of extracellular collagen and the development of fibrosis [33]. T- and B-lymphocyte infiltration suggests that chronic inflammation [26] contributes to myocardial fibrosis in response to injury [34]. Further supporting the association between inflammation and fibrosis, a strong correlation between the level of leukocyte infiltration and fibrosis in the LA 28 days after insular ischemic stroke was identified.

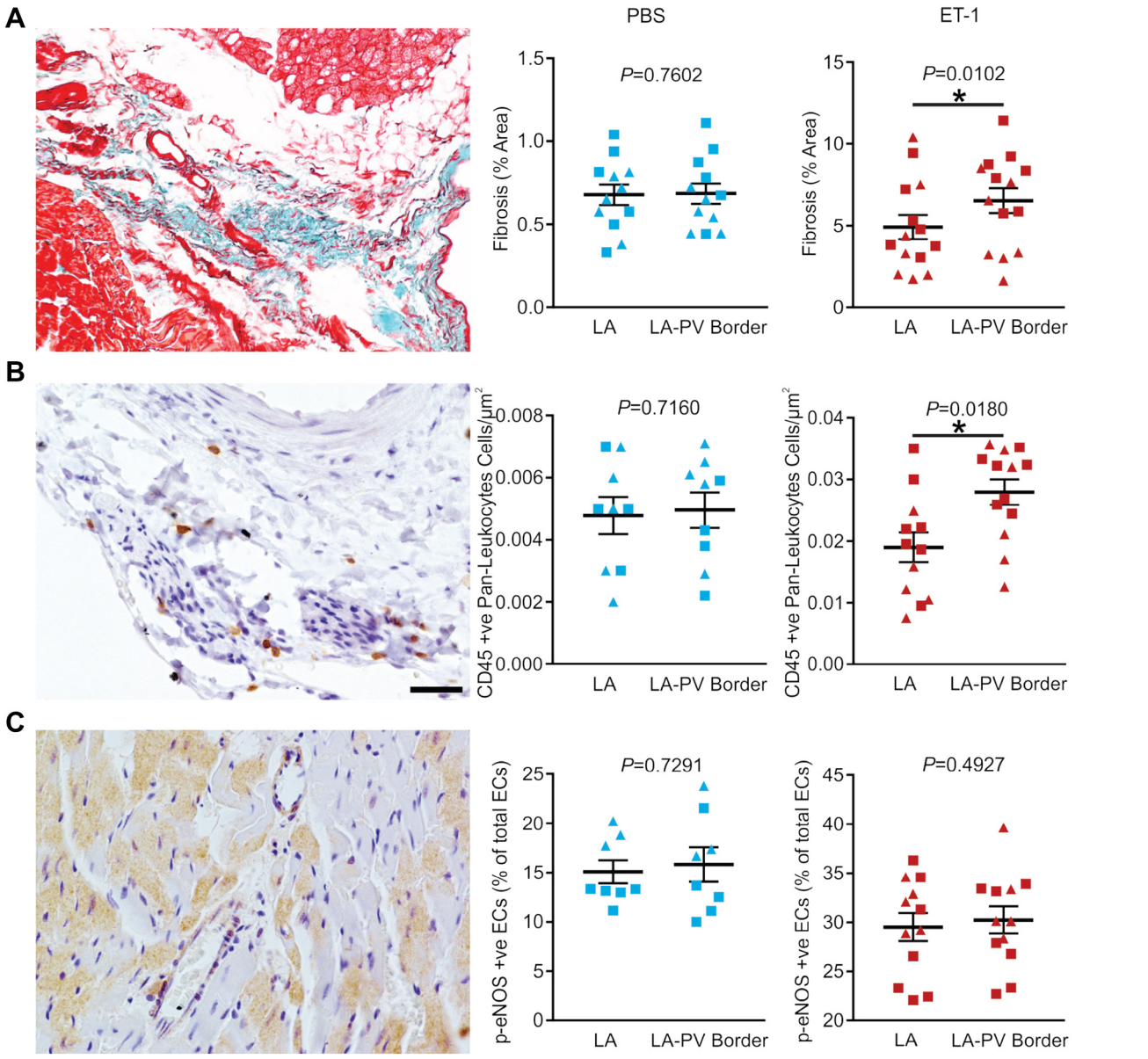

Fig. 4. Enhanced inflammatory infiltration and fibrosis at the LA-PV border. (A) Representative photomicrograph of the LA-PV border 28 days following induced insular stroke, with increased fibrotic area in ET-1 injected rats (n = 14) between LA and LA-PV border. (B)Representative photomicrograph of LA-PV border 28 days following insular stroke, with increased pan-leukocyte infiltration following selective insular stroke (n = 14). (C)Representative photomicrograph of the LA-PV border 28 days following induced insular stroke, with no significant differences in phosphorylated eNOS activation for both control (n = 12; left) and ET-1 injected rats (n = 14; right) between LA and LA-PV border. Data is represented as group mean ± SEM; *indicates statistical significance via Student's t-test.

Supporting our findings, previous studies have shown a correlation between the amount of cardiac collagen and inflammatory cells in patients with cardiac dysfunction [35].

Based on the well-known role of atrial fibrosis in the genesis of cardiac arrhythmias, the observed LA fibrosis in left and right insular stroke rats may constitute a contributing factor to the development and progression of neurogenic atrial fibrillation in patients with acute insular infarcts [2]. Similarly, it may favor the development of life-threatening cardiac arrhythmias resulting in sudden cardiac death after stroke [36], although this remains to be proven in future experimental models. Studies investigating the incidence of cardiac arrhythmias after selective insular ischemic stroke are needed for establishing a definite correlation between LA histopathological changes and arrhythmogenesis.

Fibrosis, pan-leukocyte infiltration, and phosphorylated eNOS activation were increased in the LA of either left or right insular stroke rats compared to PBS, with no apparent lateralization. Although autonomic cardiac tone appears to be lateralized at the level of the insular cortex [37], cardiac dysfunction downstream of the insula involving local inflammation from myocardial nerves [7] may be indistinguishable. In humans, data on stroke-induced cardiac injury are conflicting, pointing alternatively to the right [38], left [39], both insular cortices considered together [40] or separately [41], or none [42]. Left atrial changes seem to be related to imbalance of sympathetic and parasympathetic activity rather than being triggered by either one or the other component or left vs. right insular cortex damage [2,43].

As the insular cortex plays a central role in autonomic control [37], we measured the level of inflammation at a region with high autonomic innervation, specifically the LA-PV border, and found that the observed pathology was enhanced in this region following selective insular stroke. This finding highlights the possibility that the LA pathology

observed in our model stems from local inflammation triggered by preganglionic fibers ending in the ganglionated plexi [44]. Autonomic dysfunction has been implicated in cardiac damage, as activation of the sympathetic nervous system may induce myocardial inflammation [45]. The loss of autonomic control could impair the inflammatory reflex, hindering the suppression of unwanted inflammation at sympathetically innervated regions of the heart [46]. It is unclear if this mechanism exists on its own or in addition to systemic inflammation induced via the initial cerebrovascular injury.

Troponin T, an early diagnostic marker of myocardiocyte necrosis [17], did not reveal differences between groups either. Importantly, these findings suggest that fibrosis is not mediated by myocardiocyte necrosis. Rather, it is more likely to be mediated through non-ischemic mechanisms such as local MII. As an alternative explanation, more recent evidence suggests that elevated troponin I and T levels in humans are a marker of pre-stroke, sometimes subclinical, heart and vascular disease, rather than a consequence of stroke-associated heart injury [47]. Supporting this hypothesis, elevated troponin levels have been only associated with cardioembolic mechanisms but not with other subtypes of ischemic stroke [48]. No differences in LA area or diameter were evident following focal ischemic stroke in the rats. We hypothesize that the time between stroke induction and the assessment of LA size (28 days) was relatively short, perhaps not enough for the LA fibrosis to result in significant chamber sizes changes. Future studies evaluating LA size changes at longer time windows are needed. The time-course analysis of BNP, a cardiac peptide secreted in response to myocardial wall stress stimulation [16], revealed no differences between insular stroke groups and controls. BNP is mostly secreted in the ventricles, although the atria also contribute. Additionally, the lack of BNP elevation may be explained by the lack of left atrial enlargement. Whether BNP is elevated at later stages of stroke-associated heart injury remains to be evaluated.

The present findings describe a novel model of left atrial cardiopathy induced by selective insular ischemic stroke. Our data suggests that ischemic stroke confined to the insular cortex is sufficient to induce left atrial cardiopathy, including LA CMED, MII, and fibrosis. Furthermore, certain pathological features are enhanced at the LA-PV border within the heart, indicating a potential role for autonomic dysfunction in producing cardiac damage. Importantly, this proof of concept study could be regarded as a first step towards identifying novel targets for the prevention of stroke induced LA structural changes and possibly post-stroke cardiovascular complications such as cardiac arrhythmias and coronary events. However, further research is needed to achieve this goal. Future investigations should also focus on the time-course occurrence of insular stroke-induced LA cardiopathy, on changes occurring in the ventricles and right atrium, and on myocardial changes occurring after larger MCA ischemic strokes or infarcts of similar sizes involving other brain areas. Considering that 44% of deaths after stroke have a cardiovascular cause [49] and that stroke causes 3.3 million deaths worldwide each year [50], we estimate that 1.5 million people die of post-stroke cardiovascular complications around the world yearly. But this is only the tip of the iceberg. Multiple other cardiovascular complications have been described after stroke. Better understanding how heart disease occurs after stroke may allow for the identification of specific treatable (e.g., anti-inflammatory drugs, beta-blockers) pathophysiological mechanisms [29].

Author contributions

BB, VJ, and VT carried out the experiments. BB, VJ, VT, SNW, and LAS contributed to study design, and reviewed and revised the manuscript. BB, VJ, VT, SNW, and LAS analyzed and interpreted the data. BB, VJ, SNW, and LAS wrote the manuscript. SNW and LAS acquired funding for the study. LAS designed and supervised the study.

Declaration of Competing Interest

LAS has received research support from Boehringer Ingelheim; speaker honoraria from Boehringer Ingelheim and Pfizer; and consulting fees from β Innovation and Bayer.

Acknowledgements

We are grateful for the staff at the Animal Care and Veterinary Services at The University of Western Ontario, and to Lynn Wang, Caroline O'Neil and Shannon Seney for their technical assistance.

Sources of funding

This work was supported by CIHR, CCNA and CFI operating and infrastructure grants to SNW; Lawson Health Research Institute Internal Research Fund to VT; as well as the Kathleen & Dr. Henry Barnett Research Chair in Stroke Research (Western University, London, Ontario, Canada), the Western University Medical and Health Sciences Board Research Seed Grant, and the Edward and Alma Saraydar Neurosciences Fund (London Health Sciences Foundation), and the Opportunities Fund of the Academic Health Sciences Center Alternative Funding Plan of the Academic Medical Organization of Southwestern Ontario (AMOSO) to LAS.

Appendix A. Supplementary data

Supplementary data to this article can be found online at https://doi.org/10.1016/j.ijcard.2019.06.004.

References

[1] L.A. Sposato, L.E. Cipriano, G. Saposnik, E. Ruiz Vargas, P.M. Riccio, V. Hachinski, Diagnosis of atrial fibrillation after stroke and transient ischaemic attack: a systematic review and meta-analysis, Lancet Neurol. 14 (2015) 377–387.
[2] L.A. Sposato, P.M. Riccio, V. Hachinski, Poststroke atrial fibrillation: cause or consequence? Critical review of current views, Neurology 82 (2014) 1180–1186.
[3] Sposato LA, Fridman S, Whitehead SN, Lopes RD. Linking Stroke-Induced Heart Injury and Neurogenic Atrial Fibrillation: A Hypothesis to be Proven. J Electrocardiol. 2018;pii:S0022–0736(18)30097–9.
[4] D.F. Cechetto, J.X. Wilson, K.E. Smith, D. Wolski, M.D. Silver, V.C. Hachinski, Autonomic and myocardial changes in middle cerebral artery occlusion: stroke models in the rat, Brain Res. 502 (1989) 296–305.
[5] P.M. Mertes, J.P. Carteaux, Y. Jaboin, et al., Estimation of myocardial interstitial norepinephrine release after brain death using cardiac microdialysis, Transplantation. 57 (1994) 371–377.
[6] K.S. Butcher, D.F. Cechetto, Insular lesion evokes autonomic effects of stroke in normotensive and hypertensive rats, Stroke. 26 (1995) 459–465.
[7] I.J. Elenkov, R.L. Wilder, G.P. Chrousos, E.S. Vizi, The sympathetic nerve—an integrative interface between two supersystems: the brain and the immune system, Pharmacol. Rev. 52 (2000) 595–638.
[8] J.S. Pober, W. Min, J.R. Bradley, Mechanisms of endothelial dysfunction, injury, and death, Annu. Rev. Pathol. 4 (2009) 71–95.
[9] J.S. Pober, W.C. Sessa, Inflammation and the blood microvascular system, Cold Spring Harb. Perspect. Biol. 7 (2014) a016345.
[10] F.L.Y. Yang, X.P. Yang, J. Xu, A. Kapke, O.A. Carretero, Myocardial infarction and cardiac remodelling in mice, Exp. Physiol. 87 (2002) 547–555.
[11] T. Wynn, Cellular and molecular mechanisms of fibrosis, J. Pathol. 214 (2008) 199–210.
[12] J.G. Travers, F.A. Kamal, J. Robbins, K.E. Yutzey, B.C. Blaxall, Cardiac fibrosis: the fibroblast awakens, Circ. Res. 118 (2016) 1021–1040.
[13] P. Gal, N.F. Marrouche, Magnetic resonance imaging of atrial fibrosis: redefining atrial fibrillation to a syndrome, Eur. Heart J. 38 (2017) 14–19.
[14] L.A.C.G. Sposato, J.M. Wardlaw, P. Sandercock, R.I. Lindley, V. Hachinski, Effect of right insular involvement on death and functional outcome after acute ischemic stroke in the IST-3 trial (third international stroke trial), Stroke 47 (2016) 2959–2965.
[15] F. Colivicchi, A. Bassi, M. Santini, C. Caltagirone, Prognostic implications of right-sided insular damage, cardiac autonomic derangement, and arrhythmias after acute ischemic stroke, Stroke 36 (2005) 1710–1715.
[16] M. Weber, C. Hamm, Role of B-type natriuretic peptide (BNP) and NT-proBNP in clinical routine, Heart 92 (2006) 843–849.
[17] L. Babuin, A.S. Jaffe, Troponin: the biomarker of choice for the detection of cardiac injury, CMAJ 173 (2005) 1191–1202.

[18] S. Jalini, R. Rajalingam, R. Nisenbaum, A.D. Javier, A. Woo, A. Pikula, Atrial cardiopathy in patients with embolic strokes of unknown source and other stroke etiologies, Neurology 92 (2019) e288–e294.
[19] Tatsuya Kawasaki CS, Kuniyasu Harimoto, Michiyo Yamano, Shigeyuki Miki, Tadaaki Kamitani. Usefulness of high-sensitivity cardiac troponin T and brain natriuretic peptide as biomarkers of myocardial fibrosis in patients with hypertrophic cardiomyopathy. Am. J. Cardiol. 2013;112:867–872.
[20] W.A. Jacob, A. Van Bogaert, M.H. De Groodt-Lasseel, Myocardial ultrastructure and haemodynamic reactions during experimental subarachnoid haemorrhage, J. Mol. Cell. Cardiol. 4 (1972) 287–298.
[21] A.Y. Tan, H. Li, S. Wachsmann-Hogiu, L.S. Chen, P.S. Chen, M.C. Fishbein, Autonomic innervation and segmental muscular disconnections at the human pulmonary vein-atrial junction: implications for catheter ablation of atrial-pulmonary vein junction, J. Am. Coll. Cardiol. 48 (2006) 132–143.
[22] L.G. Luna, Manual of the Histologic Staining Methods of the Armed Forces Institute of Pathology, 3rd edition McGraw-Hill Book Co, New York, 1968.
[23] Kenneth S. Butcher, John X. Wilson VCH, Collete Guiraudon, David F. Cechetto, Cardiac and sympathetic effects of middle cerebral artery occlusion in the spontaneously hypertensive rat, Brain Res. 621 (1993) 79–86.
[24] M.A. Samuels, The brain-heart connection, Circulation. 116 (2007) 77–84.
[25] K.J. Tracey, The inflammatory reflex, Nature 420 (2002) 853–859.
[26] F.K. Swirski, M. Nahrendorf, Leukocyte behavior in atherosclerosis, myocardial infarction, and heart failure, Science (New York, NY) 339 (2013) 161–166.
[27] H. Qi, S. Yang, L. Zhang, Neutrophil extracellular traps and endothelial dysfunction in atherosclerosis and thrombosis, Front. Immunol. 8 (2017) 928.
[28] B. Olshansky, Vagus nerve modulation of inflammation: cardiovascular implications, Trends Cardiovasc. Med. 26 (2016) 1–11.
[29] J.O. Cerasuolo, L.E. Cipriano, L.A. Sposato, The complexity of atrial fibrillation newly diagnosed after ischemic stroke and TIA: advances and uncertainties, Curr. Opin. Neurol. 30 (2017) 28–37.
[30] M. Acampa, P.E. Lazzerini, F. Guideri, R. Tassi, A. Lo Monaco, G. Martini, Inflammation and atrial electrical remodelling in patients with embolic strokes of undetermined source, Heart Lung Circ. 28 (2019) 917–922.
[31] J.H. Greenhoot, D.D. Reichenbach, Cardiac injury and subarachnoid hemorrhage. A clinical, pathological, and physiological correlation, J. Neurosurg. 30 (1969) 521–531.
[32] K.K. Gupta, D.L. Donahue, M.J. Sandoval-Cooper, F.J. Castellino, V.A. Ploplis, Plasminogen activator inhibitor-1 protects mice against cardiac fibrosis by inhibiting urokinase-type plasminogen activator-mediated plasminogen activation, Sci. Rep. 7 (2017) 365.
[33] A. Nicoletti, J.B. Michel, Cardiac fibrosis and inflammation: interaction with hemodynamic and hormonal factors, Cardiovasc. Res. 41 (1999) 532–543.
[34] T.A. Wynn, Cellular and molecular mechanisms of fibrosis, J. Pathol. 214 (2008) 199–210.
[35] D. Westermann, D. Lindner, M. Kasner, et al., Cardiac inflammation contributes to changes in the extracellular matrix in patients with heart failure and normal ejection fraction, Circ. Heart Fail. 4 (2011) 44–52.
[36] F.L. Silver, J.W. Norris, A.J. Lewis, V.C. Hachinski, Early mortality following stroke: a prospective review, Stroke. 15 (1984) 492–496.
[37] S. Meyer, M. Strittmatter, C. Fischer, T. Georg, B. Schmitz, Lateralization in autonomic dysfunction in ischemic stroke involving the insular cortex, Neuroreport. 15 (2004) 357–361.
[38] T. Krause, K. Werner, J.B. Fiebach, et al., Stroke in right dorsal anterior insular cortex is related to myocardial injury, Ann. Neurol. 81 (2017) 502–511.
[39] S. Laowattana, S.L. Zeger, J.A. Lima, S.N. Goodman, I.S. Wittstein, S.M. Oppenheimer, Left insular stroke is associated with adverse cardiac outcome, Neurology 66 (2006) 477–483.
[40] H.S. Song, Back JH, Jin DK, et al. cardiac troponin T elevation after stroke: relationships between elevated serum troponin T, stroke location, and prognosis, J. Clin. Neurol. (Seoul, Korea). 4 (2008) 75–83.
[41] J.F. Scheitz, M. Endres, H.C. Mochmann, H.J. Audebert, C.H. Nolte, Frequency, determinants and outcome of elevated troponin in acute ischemic stroke patients, Int. J. Cardiol. 157 (2012) 239–242.
[42] H. Christensen, H.H. Johannesen, A.F. Christensen, K. Bendtzen, G. Boysen, Serum cardiac troponin I in acute stroke is related to serum cortisol and TNF-alpha, Cerebrovasc. Dis. 18 (2004) 194–199.
[43] A.Y. Tan, S. Zhou, M. Ogawa, et al., Neural mechanisms of paroxysmal atrial fibrillation and paroxysmal atrial tachycardia in ambulatory canines, Circulation 118 (2008) 916–925.
[44] S.M. Oppenheimer, A. Gelb, J.P. Girvin, V.C. Hachinski, Cardiovascular effects of human insular cortex stimulation, Neurology 42 (1992) 1727–1732.
[45] H. Nguyen, J.G. Zaroff, Neurogenic stunned myocardium, Curr. Neurol. Neurosci. Rep. 9 (2009) 486–491.
[46] B. Olshansky, H.N. Sabbah, P.J. Hauptman, W.S. Colucci, Parasympathetic nervous system and heart failure: pathophysiology and potential implications for therapy, Circulation 118 (2008) 863–871.
[47] X. Jia, W. Sun, R.C. Hoogeveen, et al., High-sensitivity troponin I and incident coronary events, stroke, heart failure hospitalization, and mortality in the ARIC study, Circulation 139 (2019) 2642–2653 (Published online before print).
[48] S. Yaghi, A.D. Chang, B.A. Ricci, et al., Early elevated troponin levels after ischemic stroke suggests a cardioembolic source, Stroke 49 (2018) 121–126.
[49] J. Prosser, L. MacGregor, K.R. Lees, H.C. Diener, W. Hacke, S. Davis, Predictors of early cardiac morbidity and mortality after ischemic stroke, Stroke 38 (2007) 2295–2302.
[50] V.L. Feigin, G.A. Roth, M. Naghavi, et al., Global burden of stroke and risk factors in 188 countries, during 1990-2013: a systematic analysis for the global burden of disease study 2013, Lancet Neurol. 15 (2016) 913–924.